PERGAMON

Electrochimica Acta 44 (1999) 3769–3777

ELECTROCHIMICA Acta

Localised investigation of coarse grain gold with the scanning droplet cell and by the Laue method

Achim Walter Hassel*, [1], Masahiro Seo

Laboratory of Interfacial Electrochemistry, Graduate School of Engineering, Hokkaido University, Sapporo, Japan

Received 9 September 1998

Abstract

A coarse grain gold specimen was investigated using the scanning droplet cell (SDC). Voltamograms on single grains were obtained and show the shape which is characteristic for a (111) single crystal plane. The potential dependence of the capacity was recorded as well. The crystallographic orientation of each grain was determined by Laue X-ray back scattering. All grains have a (111) orientation but different azimuth angles. This angle was determined quantitatively for different grains. SEM micrographs show that the breadth of the grain boundaries is some 12 μm. The terraces of the grain and the grain boundaries were investigated by scanning impedance measurements using the SDC. Three different droplet diameters (50, 100 and 250 μm) were used. The grain boundary could be detected with all cells. The local capacity within the grain boundary was determined from this experiment. It is found to be 60% higher than that of the grains themselves, probably due to the enlarged area within the ditch. The structure of the specimen is discussed and a model describing the results is presented.

Keywords: Scanning droplet cell; Localised Electrochemistry; Coarse grain gold; Laue method; Gold single crystal

1. Introduction

It is well known, that the reactivity of an electrode surface can depend on its crystal orientation. Countless investigations were carried out on single crystal electrodes. Among these, gold seems to be the best investigated system. According to the giant number of papers published in this field, nowadays reviews have to focus on specific aspects such as the behaviour in the double layer region [1] or the under potential deposition [2].

These investigations have already lead to a deeper understanding of the electrochemistry of a single crystal electrode [3]. However, the behaviour of a polycrystalline electrode cannot be simply predicted from the knowledge of each orientations share on the surface and the single crystal data.

The first reason is the presence of grain boundaries which are separating the grains from each other. These boundaries behave very dissimilar from the flat quasi-single crystal grains, since their structure must be inherently a patchwork. The second reason is the interaction of neighbour grains. It is obvious that the difference in their physical properties diminish or vanish with decreasing size and distance since the corresponding gradient of this property cannot increase infinitely.

Recently the number of investigations where the heterogeneity of a polycrystalline material is the subject of interest increased steadily. One reason is nowadays availability of different scanning techniques. Among

* Corresponding author.

[1] hassel@elechem1-mc.eng.hokudai.ac.jp

0013-4686/99/$ - see front matter
PII: S0013-4686(99)00082-1

others the scanning electrochemical microscope [4], the scanning reference electrode [5], the scanning probe impedance [6], the Kelvin probe [7] and the measurement of the local electrochemical impedance using a probe with two parallel micro-electrodes [8] were employed for those studies. Even in situ optical methods like micro-ellipsometry [9] or confocal spectroscopy using IR, VIS or UV light provides new information. The application of in situ nano scale probes offers new possibilities [10] as well.

However, there is still a lack in a spatial resolved application of the classical electrochemical methods, the potential-current methods like cyclic voltametry and current transient of potentiostatic pulse steps or galvanostatic measurements, respectively.

The influence of the grain structure on the corrosion of passive iron was recently shown by Fushimi et al. [11] using SECM and an anisotropic etching method.

Another way to obtain these results were impressively demonstrated by Kudelka et al. [12]. They studied the electrochemistry of single grains of coarse grain titanium using an innovative photo resist technique combined with a small electrolyte droplet. They showed that the reactivity clearly depends on the crystallographic orientation of the grains. This method uses fixed single spots on the electrode and cannot map the whole surface. In some cases, if the treatment during the production of the micro electrodes modifies the surface, this method may not be applicable.

A novel method, named scanning droplet cell [13] (SDC) overcomes some of the above mentioned limitations. Its application had been demonstrated by means of structured oxide films on aluminium [14].

This method will be used for the investigation of gold, here.

2. Experimental

2.1. Chemical

All solutions were prepared from reagent grade chemicals and ultrapure water. The latter was prepared from *aqua bidestillata* which was redistilled from $KMnO_4$ and finally cleaned with a Millipore Q filter system. The specific resistance was higher than 16.8 MΩ cm (25°). 1 mol l^{-1} perchloric acid was used as electrolyte.

A miniaturised Ag/AgCl/sat.-KCl reference electrode was used in connection with a KNO_3 salt bridge. Its potential and stability was checked against a commercial type Ag/AgCl/sat.-KCl reference electrode. The potential difference between these two electrodes never exceeded a value of 3 mV, even in long time transients. Details of its construction and characterisation are given elsewhere [15].

A thin gold wire (Tanaka Kikinzoku Kogyo K.K., Tokyo, Japan) with a diameter of 100 μm and a purity of 99.997% was used as counter electrode. The gold working electrodes with coarse grains were prepared by the same company upon our request. The purity was 99.99% and the thickness was 80 μm. The sample was washed with acetone to remove the residuals of the glue which had been used during production. After washing with ethanol the sample was washed with a large amount of pure water. The specimen was then immersed into the electrolyte and cycled until a steady state voltamogram was obtained. After rinsing with water the specimen was ready for use.

2.2. Electronic equipment

Depending on the experiment either a Solartron Schlumberger 1287 electrochemical interface in combination with a Solartron Schlumberger 1255 B frequency response analyzer or a high sensitive bi-potentiostat from Hokuto Denko in combination with an NF Electronic Instruments 5610B two phase lock-in amplifier was used. The bi-potentiostat is a prototype which is not commercially available yet. However, in these experiments it was only used in the potentiostat-mode rather than in bi-potentiostat-mode.

For an effective spatial resolved investigation a Chuo Seiki x–y–z-stage was used. It was driven by a 4 channel DC motor controller with one encoder for each dimension. The reproducibility of this stage is better than 100 nm over the whole 15 mm long scan range.

To realise the coarse volume control of the SDC either a linear motor with satellite gear or a manually driven micrometer screw was combined with a syringe. One of the above-mentioned stepmotors was connected to a microliter syringe to construct a pl-pipette to be used for the fine volume control of the SDC. A nominal resolution of 9 pl is calculated for this device from the length (55 mm) and the total volume of the syringe (5 μl). It was driven by the fourth channel of the motor controller. All electronic devices were connected via the GPIB bus to a computer.

2.3. The Scanning Droplet Cell (SDC)

The scanning droplet cell produces a small electrolyte droplet at its tip and touches the area of interest with it. This defines the area of the working electrode to be investigated. This droplet is held between the surface of interest and the SDC in an equilibrium of different forces. The shape and size of the droplet are determined by the capillary forces, the weight of the droplet, the surface tension of the liquid phase which mainly depend on the composition of the electrolyte and the surface tension on the electrode being a func-

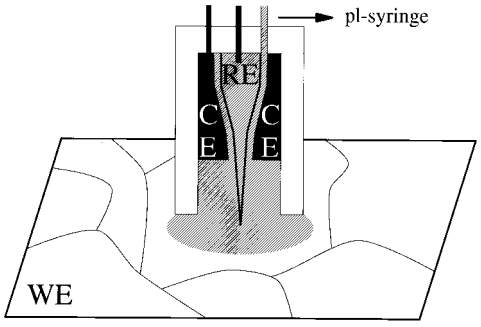

Fig. 1. Schematic presentation of the scanning droplet cell type, used in this investigation. It consists of an outer isolating glass capillary and an inner isolating concentric reference electrode capillary. The whole miniaturised reference electrode, including a salt bridge, is integrated in the droplet cell. A chemically etched gold spiral was used as a counter electrode. The diameter of the tip of the outer capillary was 50, 100 or 250 μm.

tion of the potential. They can be easily adjusted by changing the distance between capillary and specimen and by controlling the volume of the droplet. If these parameters are optimised a contact angle of about 90° can be achieved at common metal surfaces. This guarantees a very sharp demarcation of the area. Within this droplet all common electrochemical investigations like rest-potential measurement, electrochemical impedance spectroscopy, cyclic voltametry, current transients of potentiostatic pulses or galvanostatic measurements can be used [13,14]. If the distance between capillary and working electrode is optimised it becomes possible to shift the droplet and to scan the surface. Size and shape of the drop can be observed using a video microscope.

Fig. 1 shows the scanning droplet cell used for these investigations. It consists of a glass capillary with a tip diameter of 25 μm (100 μm, 50 μm). The back body of these capillary contains the counter electrode CE. A spiral made from a thin gold wire was used to achieve a large area within a small volume. It was chemically etched to increase the effective surface by roughening. A micro reference electrode with a diameter of 800 μm and a length of 15 mm was mounted within the main capillary. Its tip has a diameter of 8–50 μm and extends into the droplet like a Luggin-capillary. The front part is filled with an agar based KNO_3 solution that acts as a salt bridge. Details of the construction of this reference electrode are given in [15].

Since the droplet volume is a key parameter in this measurement, lots of effort has been made to develop a precise control of the droplet. The pl-syringe described in Section 2.2 has a sufficiently high resolution to guarantee a continuous control of the droplet volume. All measurements have been performed in a nitrogen atmosphere. Due to the extraordinary high surface/volume ratio in the droplet the dissolved oxygen is replaced by nitrogen within a few minutes.

In principle the resolution of the method scales directly with the droplet diameter. However, if the droplet is shifted in steps smaller than its diameter, the resolution can be increased to about 1/10 of the droplet diameter using a mathematical defolding procedure [13]. In the case of passive films on aluminium the normal resolution is extremely high and thickness differences of 0.2 nm can be detected [14].

2.3.1. Scanning impedance measurement

If the SDC is combined with a lock-in amplifier or a frequency response analyser the local impedance within the droplet can be measured. After shifting the droplet to another position the next data point is recorded. In this way it becomes possible to realise a scanning impedance measurement. Due to the reduced surface area the current flow related to the perturbation signal is very small. Therefore the impedance to be measured is rather high, but still capable for a 50 μm droplet on gold. A perturbation amplitude of 10 mV was used for all measurements. Since a single impedance spectra takes a comparable long time to be measured, the number of these spectra and therefore the resolution is limited by the total time available for the imaging.

2.3.2. Scanning cyclic voltametry

The scanning cyclic voltametry with a SDC was already demonstrated [14]. The main difference to these measurements are the problems to achieve a steady state cycle. It is well known that the first cycles on gold differ from the following ones. Therefore it was necessary to remain at one position on the specimen for several cycles in order to measure a satisfying local voltamogram.

2.3.3. Scanning rest potential measurement

The scanning droplet cell can be also used for scanning rest potential measurements. For these measurements the counter electrode is disconnected and the local rest potential is directly picked up by the reference electrode. A precise control of the droplet diameter or the wetted electrode area, respectively, is less important in this experiment, since the rest potential does not depend on the surface area.

2.4. Scanning electron microscopy

The SEM measurements were performed on a scanning electron microscope model JSM-T20 from JEOL, Tokyo. An acceleration voltage of 19 KV was used.

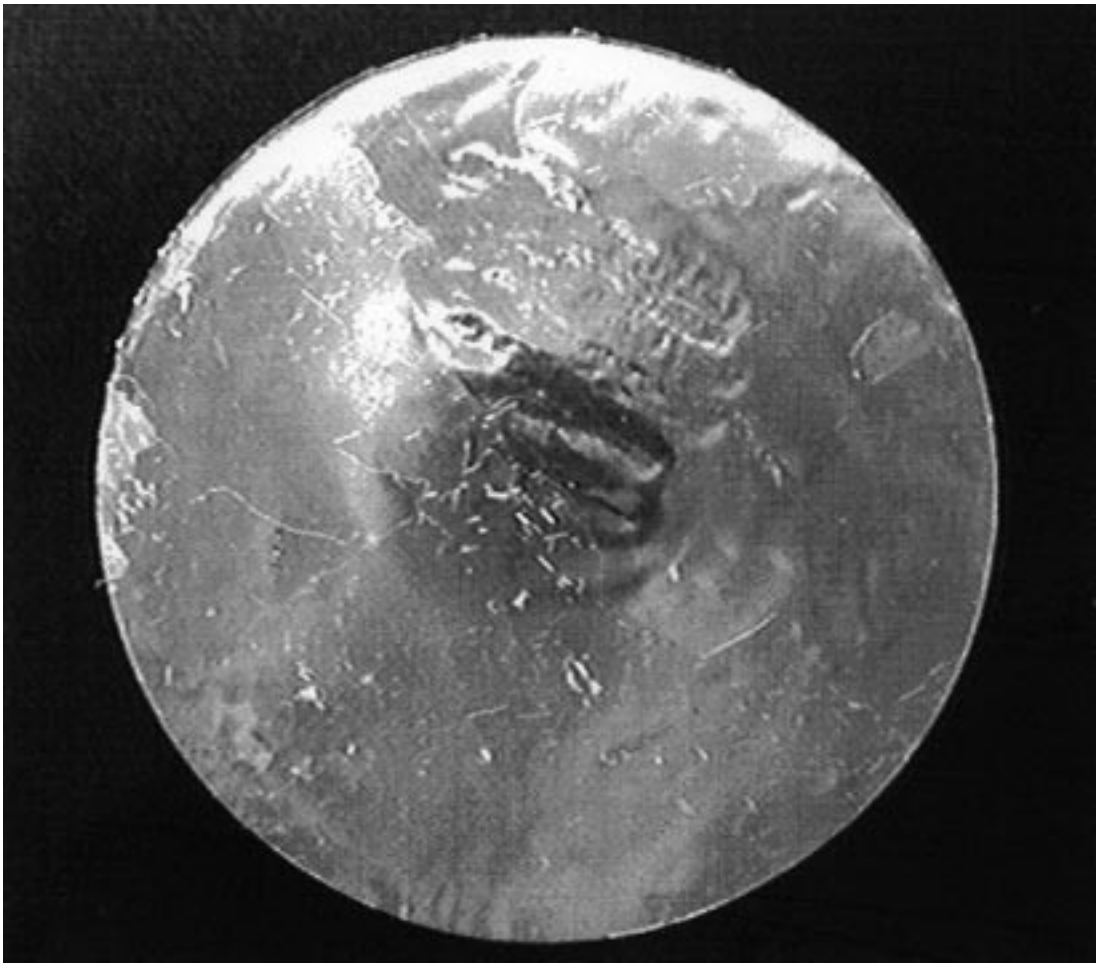

Fig. 2. Optical micrograph of the investigated coarse grain gold specimen. The diameter of the disk is 25 mm. The large dark spot in the centre is the video camera which is reflected by the sample itself.

2.5. Laue X-ray back scattering

A molybdenum cathode with a current of 20 mA at a voltage of 30 KV was used to generate the X-rays. The illuminated spot had a diameter of about 1 mm. The pictures were taken as a back reflection onto an ISO 3000 film. A special goniometer was used for adjusting the specimen. It was mounted on an x–y–z-stage, that allowed the sample to be moved relative to the X-ray beam. In this way it became possible to make the Laue analysis on each grain without changing the azimuthal or incident angle.

3. Results

3.1. Optical microscopy

Fig. 2 shows an optical micrograph of the investigated coarse grain gold specimen. The diameter of the disk was 25 mm. The dark spot in the centre is the video camera which is reflected by the sample. Some of the grain boundaries can be clearly seen. Since the reflection of each grain depends on the angle of the incident light it was not possible to take a micrograph that shows all grains and grain boundaries in the same picture. However, this picture shows clearly the huge grains with an area of some mm^2. From the presence of the visible grain boundaries one should assume different crystallographic orientations of the grains.

3.2. Scanning electron microscopy

Since the scattering of visible light is much stronger than those of electrons, the grain boundaries of the specimen had been investigated by a scanning electron microscope in order to determine the width of the boundaries. Fig. 3(a) shows a micrograph of a three

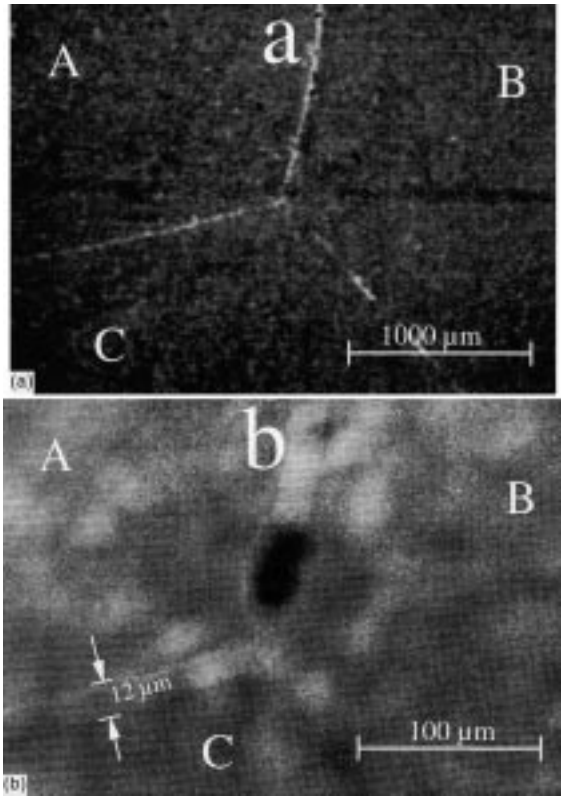

Fig. 3. SEM images of a three grain border. Two different magnifications (a) and (b) of the same position are shown. The corresponding scales are given as inserts. The borderline is about 12 µm wide, as indicated in (b).

grain border where the angle between two boundaries is about 120°. Fig. 3(b) shows the same area at a 10 times higher magnification. The grain boundaries are some 12 µm wide and the borderlines are almost straight lines. The width of the boundary is considerably constant. Near the meeting point of the boundaries a dark spot can be seen. Most of the three grain corners showed such a dark spot. Even electrons will be scattered at the grain boundaries, but the effect is less pronounced compared with visible light. Therefore, in Fig. 3(a) it seems wider, taking the magnification factor into account. This scattering is less pronounced at higher magnifications. At a magnification of 200 or higher the width of the line directly scales with the magnification factor, and hence, its determination from this microscopical method becomes reliable.

From a single picture it is not possible to decide dependably, whether a darker area originates from an elevation or a depression. The reflectivity depends also on the nature of the surface. However, if the focus of the electron beam is changed during measurement it becomes possible to determine the absolute height

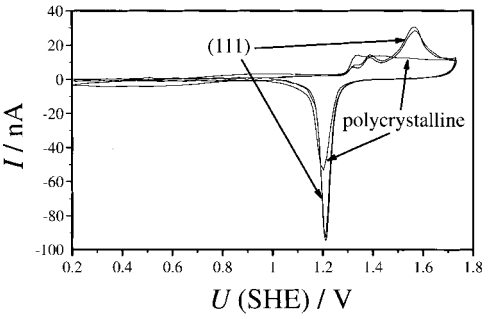

Fig. 4. Cyclic voltamograms on single grains of the coarse grain gold specimen (111). A cyclic voltamogram on a fine grain gold specimen (polycrystalline) is given for comparison. All voltamograms were obtained using a 520 µm SDC at a sweep rate of $dU/dt = 10$ mV s^{-1}.

difference. From these kind of measurements it was found that the lighter lines which refer to the boundaries as well as the dark spot are depressions. Where, in the case of the boundary, this depression appears lighter than the terrace of the grain, the small pit appears black. The depth of the boundaries could be roughly determined to be 5 µm. This method is not very precise, but the relative error should be smaller than 20% since absolute height differences of 1 µm can be clearly distinguished. A reliable determination of the depth of the pit was not possible, due to the high aspect ratio, but it clearly exceeds 20 µm.

If we assume an elliptic cross-section of the boundary we can calculate the increase of the electrochemical active area. For a given height h and diameter d the elliptic integral for the calculation of the lower half of the ellipsoids circumference L can be approximated by

$$L \approx \frac{\pi}{4}\left[\frac{3}{2}(2h + d) - \sqrt{2hd}\right] \quad (1)$$

Using $h = (5 \pm 1)$ µm and $d = 12$ µm, L has a length of (17.3 ± 1.6) µm which means an increase of (45 ± 12)%. The area increases accordingly.

3.3. Scanning cyclic voltametry

In order to characterise the electrochemical behaviour of single grains, cyclic voltametry was performed on different grains. Fig. 4 shows cyclic voltamograms on two different grains which had been recorded at a sweep rate of 10 mV s^{-1} using a 250 µm droplet. The steady state voltamograms which were obtained after several cycles are presented here. From macroscopic measurements on gold it is well known, that impurities which adhere to the surface will be electrochemically destroyed or simply removed. To guarantee that the whole area to be investigated by the droplet is cleaned

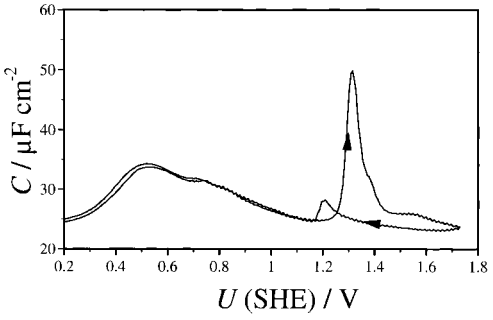

Fig. 5. Capacity as a function of the potential on a single gold grain. The scan direction is indicated by arrows. The scan rate was $dU/dt = 10$ mV s^{-1}.

in this way, a 30% larger droplet was used for the preceding cycles. After the pre-treatment the cell was moved to an outer position where the impure electrolyte was measured out. Some fresh electrolyte was then dosed to form an electrolyte droplet of the capillaries diameter, i.e. 250, 100 and 50 μm.

The voltamograms look essentially the same on all grains. The two maxima are observed in the anodic sweep. Similar curves were reported by many other authors for single crystals of gold with a crystallographic orientation of (111). Among others, the work of Dickertmann et al. [3]. Hemlin et al. [16–18] and Motheo et al. [19] may be named here. Even though, there are small discrepancies to the results obtained from massive single crystals one would identify the surface clearly as near-(111) oriented. The small deviations mentioned before, may be attributed to the different surface pre-treatment, to the different sweep rate and to the different electrolyte composition or concentration, respectively. The differences between the two grains are probably due to a slightly different droplet diameter, which results in an accordingly higher current. A comparison of the charge, consumed in these experiments, show a difference of 4%.

For comparison a cyclic voltamogram of a polycrystalline fine grain gold specimen was recorded under the same conditions. As expected, the difference is dramatic. The shape of the anodic sweep is completely different, the reduction peak is broader, less high and occurs at a slightly lower potential.

So far, from an electrochemical view all grains of the sample are expected to be (111) oriented.

3.4. Potential dependence of the capacity

Fig. 5 shows the potential dependence of the capacity of a single grain. Again, the data were recorded using the SDC with a droplet diameter of 250 μm. The capacity was calculated from the impedance, measured at 1030 Hz with a sweep rate of 10 mV s^{-1}. This experiment was carried out after achieving a steady state voltamogram.

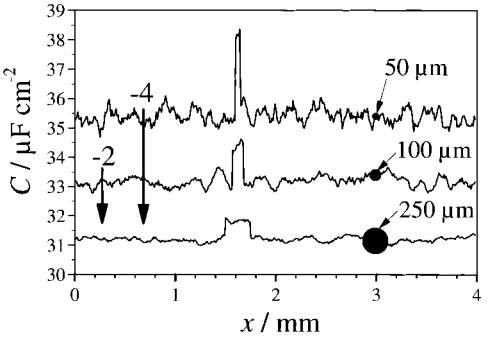

Fig. 6. Impedance scan over two grains and the separating grain boundary, at 1030 Hz with a step width of 10 μm. Three different droplet diameters (250, 100, 50 μm) were used, as indicated by the true to scale circles at $x = 3$ mm. The curves for the 100 and 50 μm droplet were shifted vertically by 2 or 4 μF cm^{-2} for reasons of clearness.

The capacity is at least 25 μF cm^{-2}. At 0.5 V a relative maximum in the capacity curve is observed, which is almost independent on the scan direction. The strongest differences between anodic and cathodic sweeps are observed when the oxide is formed or reduced. At a potential of 0.7 V a small plateau is observed. This potential was chosen in the next experiment.

3.5. Scanning impedance measurement

Fig. 6 shows the normalised capacity as a function of the position x. For this experiment a scan with the SDC was performed from one grain to the next over a grain boundary. The same scan was carried out with three different droplet cells and droplet sizes, respectively. The impedance at 1030 Hz was measured for each 10 μm step. The droplet diameters were 250, 100 and 50 μm. In order to achieve a more lucid presentation the curves for the 100 and 50 μm droplet were shifted vertically by 2 or 4 μF cm^{-2}, respectively. A true to scale indication of the droplet size is given for each curve at $x = 3$ mm.

Table 1
Numerical results of the impedance scans of Fig. 6

	50 μm	100 μm	250 μm
Overall average capacity/μF cm^{-2}	31.43	31.21	31.23
As presented in Fig. 6	35.43	33.21	31.23
Average peak capacity/μF cm^{-2}	34.17	32.41	31.82
As presented in Fig. 6	38.17	34.41	31.82
Peak centre position/mm	1.63	1.63	1.62
Peak breadth/μm	50	100	230

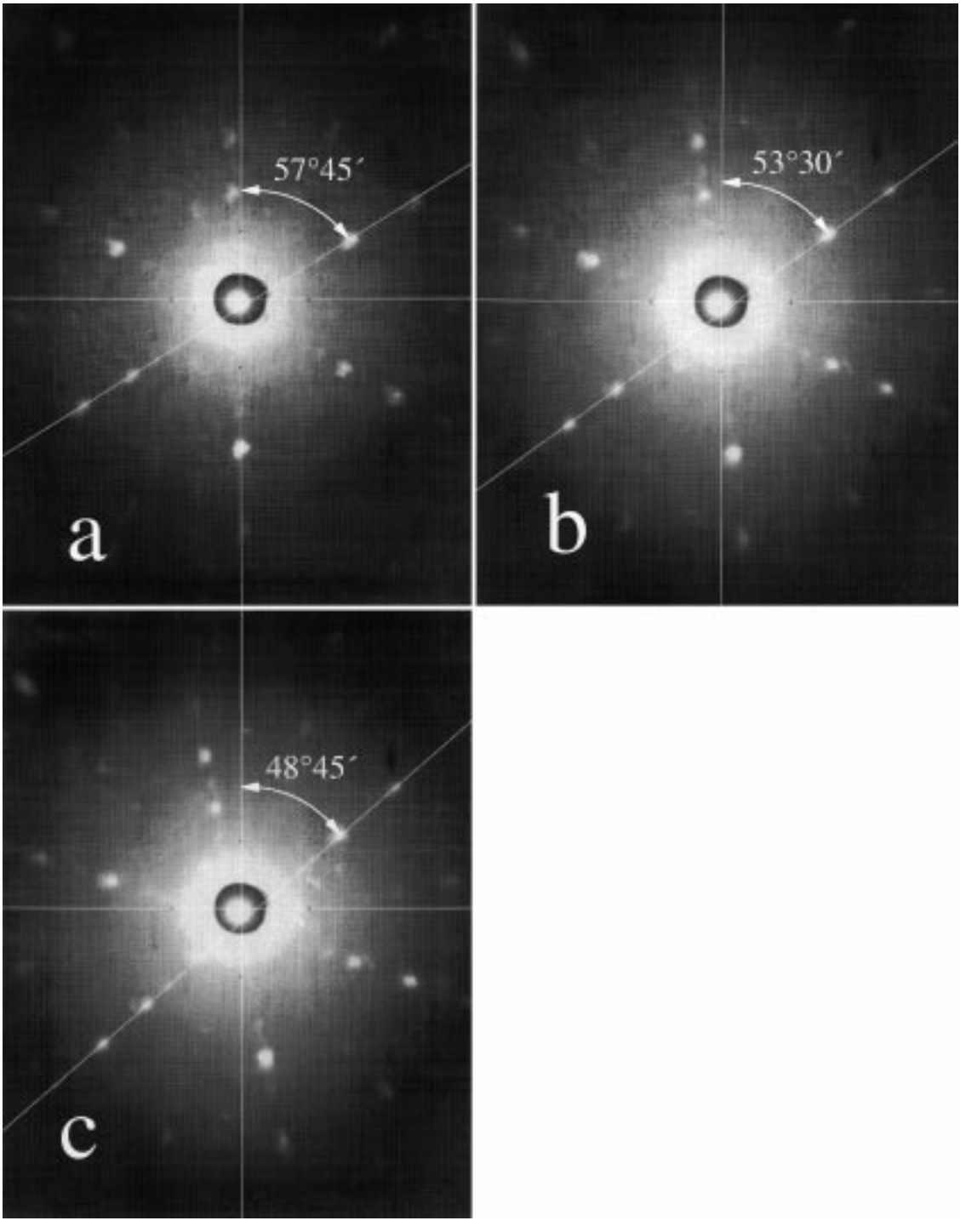

Fig. 7. Laue X-ray reflection images of three adjacent grains of the gold specimen. The thin white lines drawn through the small black spots near the centre are the Cartesian coordinates. The pattern refers to a (111) oriented face of a cubic system. The azimuth angle can be taken from the angle between a Cartesian coordinate and the thin white line drawn through the pattern.

All three curves show clearly a maximum near $x = 1.6$ mm. For a large droplet diameter the peak is broad and flat and for smaller droplets it becomes smaller and sharper. The numerical results from this figure are summarised in Table 1.

To avoid any misunderstanding, the data of the vertically shifted curves are given as well. The centre position is independent of the droplet diameter. The breadth of the peak on the other hand, depends clearly on this diameter. Since the droplet averages the impedance in its contact area, a small structure, like the 12 μm wide grain boundary, will influence the result as long as a part of the droplet covers it. From this point of view it is not surprising that the ostensible breadth given in Table 1 directly scales with the droplet diameter. Even from the relative height it is obvious that the signal is smeared out.

Hassel and Lohrengel [14] demonstrated with oxide films on aluminium, that a mathematical defolding procedure can extract the data from these raw results. Using this procedure, one obtains a 60% increase of the capacity for the grain boundary compared with the terraces. This value is slightly higher than expected from the area increase of Section 3.2. This might be attributed to an increase of the surface energy resulting from the higher degree of disorder at this borderline or simply a higher roughness within the grain boundary.

These assumptions are supported by the scanning rest potential measurement which was conducted. The result was much less pronounced compared with the impedance. No significant difference could be detected. It seems that the grain boundary does not influence the rest potential at all.

3.6. Laue X-ray scattering

To confirm the electrochemical result, that all grains have a crystallographic orientation near-(111), localised X-ray investigations on single grains were performed. The Laue method provides a simple and reliable procedure to determine the crystallographic system and orientation. Since the crystallographic system of the investigated material is already known to be the cubic system, it is not necessary to take different pictures from different directions, as it is necessary for more complex crystals. In the case of the cubic system the Laue projections have a very high symmetry and are rather simple to interpret. A brief description of this method for the characterisation of gold single crystals was given by Hamelin [1].

Fig. 7(a–c) show the X-ray back-scattering pattern of three adjacent grains. All show clearly a threefold symmetry. This symmetry is characteristic for the (111) plane of a cubic system. Four small black spots can be seen near the centre. These markers were produced by the camera and allowed to span a Cartesian coordinate system, as it is done by the small white lines in the figures. If the symmetry centre of the pattern coincide with the origin of this coordinate system, the crystallographic orientation is exactly (111). The small deviations from this coincidence indicate, that the plane is slightly tilted or the surface is a high index plane which is near-(111) such as (998). Using a Greninger chart, the exact index or the exact tilting angle, respectively, can be determined. However, in this case the angle is less than 2°. Hence, it can be neglected if the specimen is discussed in terms of cyclic voltametry and capacity measurement. If an over-structure of an adsorbed species is the subject of interest that may not be the case.

It is conspicuous that the pattern does not coincide exactly. In fact they are slightly rotated, and this angle of rotation is the so-called azimuth angle. For the three patterns shown in Fig. 7 it takes (clockwise) values of (a) 57°45′, (b) 53°30′ and (c) 48°45′. The meaning of these results will be discussed in the following section.

4. Discussion

In this work we investigated a coarse grain gold specimen. Coarse grain materials fill a gap between single crystals and polycrystalline materials. Some of the properties can be derived from the single crystals, but with decreasing grain size the interaction becomes stronger and more important.

The optical micrographs and the scanning electron micrograph show the presence of different grains, which are clearly separated from each other by grain boundaries. The grain boundaries are some 12 μm wide.

The investigation of single grains by localised cyclic voltametry with a scanning droplet cell, show reproducibily a voltamogram which is characteristic for a single crystal. A voltamogram on a fine grain material proves this curves. Surprisingly, every grain of the specimen shows an electrochemical behaviour like a (111) single crystal. These results are confirmed by an X-ray investigation. It is found, that the grains are all (111) oriented but differ in their azimuth angle. This angle was determined quantitatively for different grains from the Laue experiments.

These results may be understood on the basis of the specimen's preparation. A thin foil is rolled from a thicker specimen. During this reforming the crystallographic planes will glide along the most dense packed and most smooth plane, which is the (111) plane. But the product of this first production step is a polycrystalline specimen, where lots of grains may be (111) oriented but probably not all. Then, the sample is heated in a vacuum for several days or weeks. This

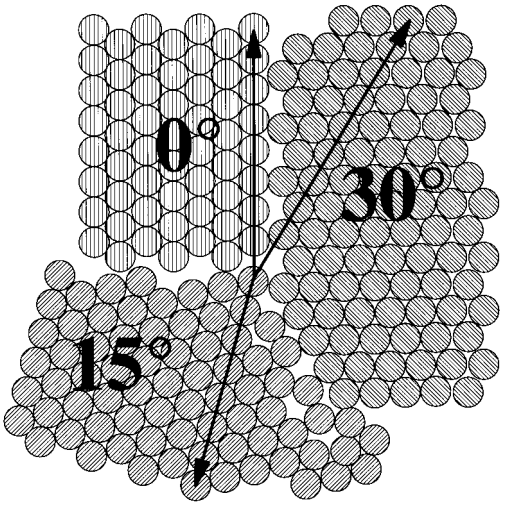

Fig. 8. Atomistic model of the coarse grain gold specimen investigated in this study. Each single grain has the (111) crystallographic orientation but different azimuth angle.

annealing increases the surface mobility of gold atoms dramatically and allows also the bulk atoms to move over a grain boundary. At that time, crystals with a low surface energy will grow, while those with a high energy will diminish, and finally vanish. As a result the (111) grains get the predominance and will supersede all other crystallographic orientations at the end. At the very end a large grain specimen with all grains being (111) oriented remains. Since the energy-win to form a single crystal is only marginal, and the activation energy for this transformation is tremendous, a steady state, which depends on the temperature, will be reached. This situation is schematically shown in Fig. 8. Three grains which are all (111) oriented, form a grain boundary similar to that found by SEM in Fig. 3. The grains are azimuthal rotated.

From an electrochemical point of view the azimuth angle has no influence, only the contribution of the grain boundaries may cause differences. As an example the capacity was investigated as a function of the position. The results show clearly the influence of the grain boundary, which increases the capacity. This may be simply an effect of roughness, but it may be some energetic effect as a result of the higher disorder as well.

The resolution of all three scanning droplet cells is sufficiently high, to measure the change in capacity caused by the 12 μm wide grain boundary. However, the smaller the droplet diameter is, the more pronounced are the changes.

Acknowledgements

The financial support of the Japan Society for the Promotion of Science and the Alexander von Humboldt-Stiftung through a postdoctoral fellowship and the Monbusho through the Grant in Aid for JSPS Fellows is gratefully acknowledged. We are indebted to Mr. Eiji Sakuma, Tanaka Kikinzoku Kogyo K.K., Tokyo for preparing the coarse grain gold specimen. Finally, we would like to thank Dr. Higuchi, Hokkaido University for making available the Laue camera.

References

[1] A. Hamelin, Mod. Aspects Electrochem. 16 (1985) 1.
[2] A. Aramata, Mod. Aspects Electrochem. 31 (1997) 181.
[3] D. Dickertmann, J.W. Schultze, K.J. Vetter, Electroanal. Chem. Interfac. Electrochem. 55 (1974) 429.
[4] A.J. Bard, G. Denault, C. Lee, D. Mandler, D.O. Wipf, Acc. Chem. Res. 23 (1990) 357.
[5] H.S. Isaacs, G. Kissel, J. Electrochem. Soc. 119 (1972) 1629.
[6] H.S. Isaacs, M.W. Kendig, Corrosion (Houston) 36 (1980) 269.
[7] M. Stratmann, H. Strehel, Corros. Sci. 30 (1990) 681.
[8] R.S. Lillard, P.J. Moran, H.S. Isaacs, J. Electrochem. Soc. 139 (1992) 1007.
[9] A. Michaelis (1994) thesis, Verlag Shaker, Aachen, ISBN-3-8265-0230-6.
[10] A.A. Gewirth, H. Siegenthaler, Nanoscale Probe of the Solid/Liquid Interface, Kluwer, Dordrecht, Boston, London, 1995.
[11] K. Fushimi, T. Okawa, K. Azumi, M. Seo, Proc. JSCE Mater. Environ., 1998, p. 211.
[12] S. Kudelka, A. Michaelis, J.W. Schultze, Ber. Bunsenges. Phys. Chem. 99 (1995) 1020.
[13] A.W. Hassel (1997) thesis, Verlag Shaker, Aachen, ISBN 3-8265-2981-2.
[14] A.W. Hassel, M.M. Lohrengel, Electrochim. Acta 42 (1997) 3327.
[15] A.W. Hassel, M. Seo, Electrochem. Comm. in press.
[16] J. Lecoeur, C. Sella, L. Tertian, A. Hamelin, C.R. Acad. Sc. Paris Serie C 280 (1975) 247.
[17] H. Angerstein-Kozlowska, B.E. Conway, A. Hamelin, L. Stoicoviciu, Electrochim. Acta 31 (1986) 1051.
[18] A. Hamelin, J. Electroanal. Chem. 407 (1996) 1.
[19] J. Motheo, A. Sadkowski, R.S. Neves, J. Electroanal. Chem. 430 (1997) 253.